HYBRID FRACTURE/DAMAGE APPROACH

J.C.W. van Vroonhoven[1] and J.B.A.M. Horsten[2]

A new approach for the analysis of dynamic crack propagation is proposed. Characteristic features of fracture mechanics and damage mechanics are combined in a finite-element method. Elements with quarter-point nodes are used at the crack tip to describe the stress singularity. The crack itself is replaced by a zone of softening material, where continuum damage mechanics is applied. Contrary to many finite-element applications of damage mechanics, this hybrid approach does not suffer from mesh sensitivity or damage localisation. The calculated crack patterns are independent of the element size and the element orientation. This method has been applied to both 2D and 3D problems of mixed-mode fracture. Good agreement with experiments and results from the literature has been obtained.

INTRODUCTION

Both fracture mechanics and continuum damage mechanics possess certain disadvantages in finite-element applications. Since numerical methods based on fracture mechanics require frequent adaptations of the finite-element mesh and use moving-element techniques, these methods will need much computing time. On the other hand, methods based on damage mechanics suffer from sensitivity with respect to the element division and from damage localisation. Because of these complications, a combination of fracture and damage mechanics within the context of the finite-element method is investigated. This has resulted in a hybrid fracture/damage approach [1, 2] which combines the accuracy of the singular crack-tip elements in fracture mechanics and the flexibility of crack representation in continuum damage mechanics. It is then expected that the disadvantages of both theories are eliminated, while their specific benefits are retained.

[1]Philips Research Laboratories, Prof. Holstlaan 4, 5656 AA Eindhoven, The Netherlands.
[2]Philips Centre for Manufacturing Technology, Eindhoven, The Netherlands.

BASIC CONCEPTS

We focus our attention on thin plate-like structures and start with a division of the elastic body into finite elements with one element over the thickness. The crack is taken uniform over the thickness with the crack front being a straight line and with the crack surfaces being perpendicular to the middle plane of the plate. Generally, the crack may propagate at different speeds in the upper and lower surfaces of the plate or in different directions. It is assumed that these effects do not occur and that the crack front remains straight.

We use the 3D eight-node (in 2D: four-node) elements with incompatible modes (see Hughes [3]), which have adjusted stiffness and give a far better performance in bending deformation than the standard linear elements. In the vicinity of the crack front, fracture mechanics is employed and extra mid-side nodes are added. We replace the original element containing the crack front by four collapsed prismatic (in 2D: triangular) elements with the side nodes shifted to the quarter points (see Barsoum [4]). This ensures the accurate calculation of the singular stresses. Since the displacements in the crack-tip elements are interpolated by quadratic shape functions, we apply variable-node elements [3] as a transition from the singular to the linear elements. The combination of the four crack-tip elements and the eight surrounding transitional elements is called the "super-element" which translates with the moving crack front. A two-dimensional projection of this structure is shown in Fig. 1. The extra nodes (including the corner nodes of the crack-tip elements) are eliminated at the super-element level by means of static condensation [3].

Continuum damage mechanics (see Chaboche [5] and Lemaitre [6]) is used to describe the "tail" of the crack. The stress-strain relations are written as

$$\sigma = (1 - D)\, E\, \varepsilon\,, \tag{1}$$

where σ and ε are the stress and strain tensors and E is the Young's modulus of the undamaged material. The damage parameter D is chosen equal to 0.999 which results in a reduction of the effective Young's modulus by a factor 1000, either isotropically or only perpendicular to the crack surfaces (see Fig. 1). This "smeared" crack concept has more flexibility in finite-element applications than fracture-mechanics procedures which require element splitting.

DYNAMICS

The discretisation of the elastic body into finite elements leads to a differential equation for the global displacement vector $\mathbf{U}$ as function of time t, viz.

$$M \cdot \ddot{\mathbf{U}} + K \cdot \mathbf{U} = \mathbf{F}\,, \tag{2}$$

where a superposed dot is the time derivative, M and K are the global mass and stiffness matrices, and $\mathbf{F}$ is the right-hand side vector of prescribed forces.

The differential equation is solved numerically at discrete times $t_n = n\,\Delta t$ (with $n = 0, 1, 2, \ldots$) by an explicit method based on central differences. The second-order derivative is approximated by

$$\ddot{\mathbf{U}}(t_n) = \frac{\mathbf{U}(t_{n+1}) - 2\mathbf{U}(t_n) + \mathbf{U}(t_{n-1})}{(\Delta t)^2}. \quad (3)$$

The truncation error is of the order $O((\Delta t)^2)$ for time steps $\Delta t \to 0$, so that the central-difference method is second-order accurate [3]. At each time step, we calculate the acceleration vector $\ddot{\mathbf{U}}(t_n)$ from the equation (2) and, next, the displacement vector $\mathbf{U}(t_{n+1})$ from (3).

The solution of (2) can be made more efficient when we apply a so-called "lumping" technique (see Hughes [3]). The mass matrix M is replaced by the diagonal matrix M^* which contains the row sums and is defined by

$$M^*_{ij} = \begin{cases} \sum_k M_{ik}, & \text{if } i = j, \\ 0, & \text{otherwise.} \end{cases} \quad (4)$$

The errors introduced by the lumping of the mass matrix cancel the errors from the time discretisation [3]. In addition, the solution of (2) no longer requires matrix inversion. Thus, the combination of the central-difference method with the lumping technique provides an accurate and efficient time-step algorithm.

CRACK PROPAGATION

The crack-propagation criterion is based on the J-integrals. The integration contour C is chosen inside the super-element around the crack tip as illustrated in Fig. 1 by a thick solid line. For dynamic crack propagation we have

$$J_k = \int_{-h/2}^{+h/2} \int_C \left[(W + T)\, n_k - \sigma_{ij}\, n_j\, u_{i,k} \right] \mathrm{d}s\, \mathrm{d}z\,, \quad (5)$$

with $k = 1, 2$ and summation over $i, j = x, y, z$, where u_i are the displacements, n_i the components of the outward normal to C, h the plate thickness, and $W = \frac{1}{2}\sigma_{ij}\varepsilon_{ij}$ and $T = \frac{1}{2}\rho\dot{u}_i\dot{u}_i$ the elastic and kinetic energy densities.

The direction of crack propagation is determined by the direction of the J-integral vector, i.e. by $\tan\theta_P = J_2/J_1$. The speed of crack propagation is set equal to the Rayleigh wave speed c_R. This is an acceptable estimate, because the exact speed will not differ much from c_R in cases of rapid fracture. As a result, the crack increment has length $c_R\,\Delta t$, while its direction is given by the angle θ_P. Crack arrest occurs when J_1 becomes negative.

Because of the crack propagation, the mass and stiffness matrices M and K in equation (2) will depend on time t. These matrices are kept constant during one time step and are adapted to the new super-element configuration after each crack increment.

APPLICATIONS

We begin with a study of possible dependences of the calculated crack paths on the element division. A square plate loaded by uniform tensile forces or bending moments is divided into a finite-element mesh with slanted orientation. The crack paths are shown in Fig. 2 and are always accurate within one element from the theoretical (straight) path.

The second application concerns curvilinear crack growth in a single-edge notched beam (see [2] and Fig. 3). The crack starts at the bottom edge of the beam and must end at the upper edge to the right of F_1 (see Schlangen [7]). The crack path of Fig. 3 clearly satisfies this requirement.

Finally, we study crack propagation in three dimensions: the torsion of a hollow cylindrical pipe (see [2] and Fig. 4). A crack is initiated in the middle cross section of the pipe and propagates in two symmetric directions. When one half of the cross section has fractured, we observe some deviations in the crack paths and the pipe reaches the point of final collapse.

CONCLUSIONS

The hybrid fracture/damage approach combines the accuracy of the singular elements in fracture mechanics and the flexibility of crack representation in damage mechanics. An effective tool has been established for the analysis of crack propagation, within the context of the finite-element method. The necessary element-mesh adaptations during crack growth are avoided, while the inaccuracies at the point of damage increase are eliminated by the use of crack-tip elements. Dependences of the crack patterns on the element size or the element orientation have not been found. Applications to several 2D and 3D problems reveal good results for the crack-propagation direction.

REFERENCES

1. J. Horsten and J. van Vroonhoven, *In: Localized Damage III, Computer-Aided Assessment and Control,* Proceedings of the 3rd Int. Conference on Localized Damage, Udine, Italy (1994) 367–374.
2. J.C.W. van Vroonhoven, *Dynamic Crack Propagation in Brittle Materials: Analyses Based on Fracture and Damage Mechanics.* PhD Thesis, Eindhoven University of Technology, The Netherlands (1996).
3. T.J.R. Hughes, *The Finite Element Method. Linear Static and Dynamic Finite Element Analysis.* Prentice-Hall, Englewood Cliffs NJ (1987).
4. R.S. Barsoum, *Int. J. for Num. Methods in Engineering* 10 (1976) 25–37.
5. J.L. Chaboche, *ASME J. of Applied Mechanics* 55 (1988) 59–64, 65–72.
6. J. Lemaitre, *Nuclear Engineering and Design* 80 (1984) 233-245.
7. E. Schlangen, *Experimental and Numerical Analysis of Fracture Processes in Concrete.* PhD Thesis, Delft University of Technology (1993).

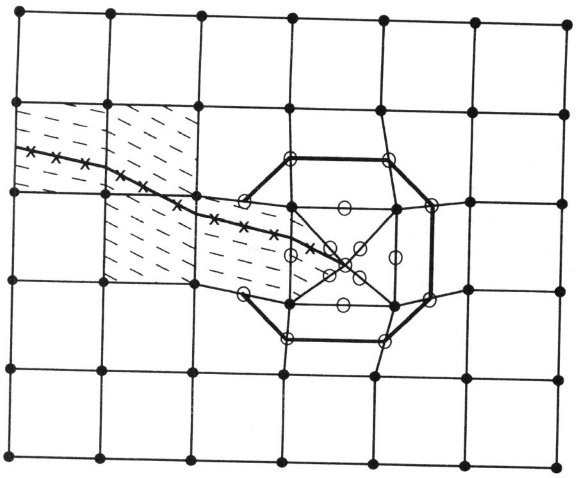

Figure 1: Configuration of the super-element and surrounding elements. Damage is displayed by dashed lines, crack path by $\times$, original nodes by $\bullet$, and extra nodes by $\circ$. Thick line indicates contour for J-integral.

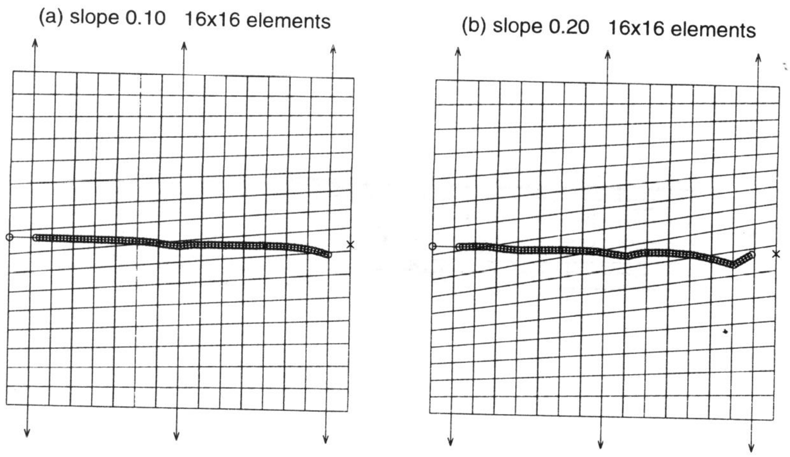

Figure 2: Crack paths in uniformly loaded square plate for various element divisions. Prospective end point of crack is indicated by $\times$.

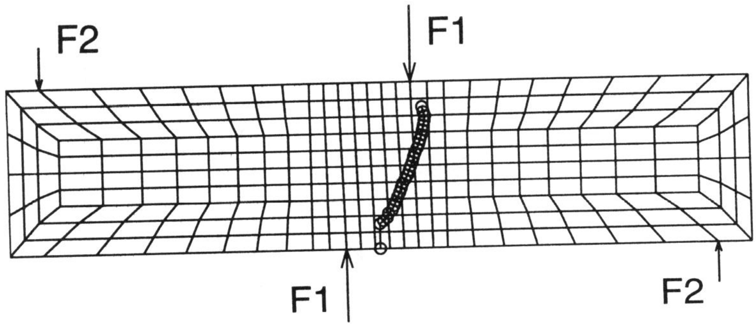

Figure 3: Crack path in single-edge notched beam in mixed-mode loading. Crack is initiated at bottom edge of beam.

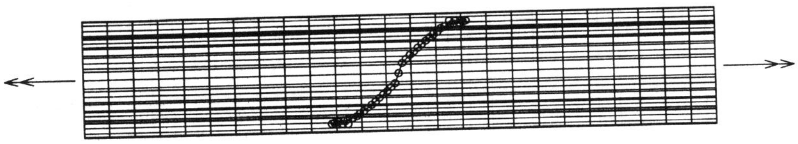

Figure 4: Crack pattern in hollow cylindrical pipe loaded by torsional moments at both end surfaces.